Cell

EXTENDED EXPERIMENTAL PROCEDURES

Identification, Sequence Analysis, and Cloning of Kinase and Scaffold Orthologs

S. cerevisiae Fus3 and Kss1 sequences were used to query the fungal orthogroups database to identify 39 Erk-like kinase sequences from across the Ascomycota. The resulting sequences were aligned using MUSCLE and adjusted manually to ensure proper alignment of critical conserved kinase features such as the DFG motif. The evolutionary history was inferred by using the Maximum Likelihood method based on the JTT matrix-based model using the MEGA5 software package to produce the tree in Figure S1A. Sequences were cloned directly from genomic DNAs or, in some cases, codon optimized forms were synthesized by Integrated DNA Technologies.

The *S. cerevisiae* Ste5 sequence was used to query the fungal orthologroups database to identify orthologous scaffold sequences. We also used BLAST to look for additional Ste5 sequences in organisms outside of those identified by the fungal orthogroups database, but did not find any additional sequences. Full-length sequences for the Ste5 orthologs we identified were cloned from genomic DNAs and served as the basis for subsequent subcloning of Ste5-FBD and Ste5-VWA sequences. A complete list of all kinase and scaffold constructs used in this study can be found in Table S1.

For identification of the Far1 and Cst5 orthologs indicated in Figure S4B, the same procedure was used as for identifying Ste5 orthologs, using the *S. cerevisiae* Far1 sequence to query Far1 orthologs and the *C. albicans* Cst5 sequence to query Cst5 orthologs.

Selection of Ste5 Fragment Sequence Boundaries

Ste5-VWA sequence boundaries were determined based on (1) sequence alignment to *S. cer.* Ste5-VWA and (2) using secondary structure prediction with SSpred to identify regions topologically congruent to Ste5-VWA.

Unlike the *S. cer.* Ste5-VWA, the *S. cer.* Ste5-FBD is a short linear motif with no obvious sequence homology present in other Ste5 orthologs. Despite this, active FBDs could hypothetically be present in these orthologs, given that linear motifs are of low sequence complexity and so can be cryptically present even in the absence of any obvious homology. We reasoned that because the *S. cer.* Ste5-FBD is found in between two easily identifiable Ste5 domains (the RING and PH domains), any functional FBD that was evolutionarily related to the *S. cer.* Ste5-FBD should also be found between these domains. As such, we identified both RING and PH domains in Ste5 scaffold sequences on the basis of both sequence alignment and secondary structure prediction with SSpred, and considered the region between the RING and PH domains of diverse Ste5 orthologs to serve as candidate FBD sequences.

Phylogenetic Analysis

The evolutionary history of Ascomycota Erk-like kinases was inferred by using the Maximum Likelihood method based on the JTT matrix-based model (Jones et al., 1992). The bootstrap consensus tree inferred from 500 replicates (Felsenstein, 1985) is taken to represent the evolutionary history of the taxa analyzed (Felsenstein, 1985). Branches corresponding to partitions reproduced in less than 50% bootstrap replicates are collapsed. The percentage of replicate trees in which the associated taxa clustered together in the bootstrap test (500 replicates) are shown next to the branches (Felsenstein, 1985). Initial tree(s) for the heuristic search were obtained automatically as follows. When the number of common sites was < 100 or less than one fourth of the total number of sites, the maximum parsimony method was used; otherwise BIONJ method with MCL distance matrix was used. The tree is drawn to scale, with branch lengths measured in the number of substitutions per site. The analysis involved 39 amino acid sequences. All positions containing gaps and missing data were eliminated. There were a total of 342 positions in the final data set. Evolutionary analyses were conducted in MEGA5 (Tamura et al., 2011).

Protein Purification

Recombinant proteins were expressed from constructs derived from previous work (pMBP, pETARA: (Reményi et al., 2005); pSV272: (Coyle et al., 2009); pFastBac-MBP: (Zalatan et al., 2012)) and were cloned by standard molecular biological techniques. Point mutants were generated by site-directed mutagenesis.

S. cerevisiae Kss1 and MBP-Ste7EE were expressed from *Spodoptera frugiperda* (SF9) cells, using the Bac-to-Bac Baculoviral Expression System (Invitrogen) at 27° as described previously (Reményi et al., 2005; Zalatan et al., 2012). Other Kss1 orthologs, Fus3 orthologs, Erk-like kinase orthologs, and Ste5 fragments were expressed and purified from *E. coli* BL21(T1R). Wild-type kinases were coexpressed with the bacterial tyrosine phosphatase YopH to ensure a homogeneously unphosphorylated activation loop tyrosine.

All constructs were purified by Ni-NTA chromatography, followed by amylose resin (for pMBP, pSV272, and pFastBac-MBP constructs) or glutathione resin (for pETARA constructs). Ion exchange (RESOURCE 15Q [Amersham], 20 mM Tris•HCl pH 8.0, 0-1M NaCl) and size exclusion chromatography (Superdex 75 10/300) were used if additional purification steps were necessary following affinity purification. Purified proteins were stored in standard buffer (20 mM Tris•HCl pH 8.0, 150 mM NaCl, 10% glycerol, and 2 mM TCEP), flash frozen, and stored at −80°.

In Vitro Kinase Reactions

Ste7→MAPK Reactions

Reactions were performed in Standard Kinase Buffer (SKB: 100 mM NaCl, 25 mM Tris pH 8.0, 0.05% NP-40, and 2 mM TCEP, 2mM $MgCl_2$) and initiated with addition of ATP to 2.0 mM. Reactions were performed under saturating concentrations of MAPK substrate

(K_M for Ste7 phosphorylation of MAPKs typically ranges between 100-250 nM) and (if present) Ste5-VWA ortholog and contained 50 nM of MBP-Ste7EE, 5 μM MAPK substrate, and (if present) 5 μM Ste5-VWA ortholog. We further verified the [MAPK] was saturating by measuring the reaction rates in the presence of 10μM MAPK; no changes to the rates were observed. Time points were quenched by the addition of 4x SDS Loading buffer that contained 50 mM EDTA. Samples were separated on 4%–12% Bis-Tris gels run in MES buffer and transferred to nitrocellulose membranes by standard methods. Western blots were performed using the 4370 anti-phospho p44/42 MAPK antibody as a primary and IRDye 800CW Goat Anti-Rabbit IgG antibody (Li-Cor #926-32211) as a secondary. Blots were visualized using the Li-Cor Odyssey Imaging System, normalized against recombinant standards for each MAPK substrate, and quantified using Odyssey 2.1 software as described previously. Kinetic constants and their errors were determined by non-linear least-squares fitting of initial rate data in R.

For the Ste5 VWA titration experiments in Figure S2A, initial rates of MAPK autophosphorylation were determined as above but contained variable amounts of the Ste5 VWA domain.

Ste5 Autoinhibition and FAB Activation Experiments

To determine the extent of autoinhibition in full-length or 'long' Ste5 fragments (constructs detailed in supplement), we measured initial rates for Ste7 → *S. cer.* Fus3 phosphorylation (under the same conditions as described for the Ste5-VWA assays) in the presence of increasing amounts of the Ste5 scaffold protein to produce an 'activation curve' (see Figure 2A) that could be fit to determine the maximal rate enhancement provided at saturation, as described previously (Zalatan et al., 2012). Activation of the autoinhibited *A. gossypii* Ste5 ortholog (*Agos*Ste5) by the SR13 Fab antibody fragment was tested by measuring initial rates for Ste7 → *S. cer.* Fus3 phosphorylation in the presence of 250 nM AgSte5 ± 2 μM SR13 Fab.

MAPK Autophosphorylation

Reactions were performed in SKB and contained 10 μM MAPK and, if present, 25 μM of a Ste5-FBD sequence. Prior to initiation with 2 mM ATP, the MAPK and the Ste5-FBD were allowed to incubate for 30 min at room temperature. Time points were quenched with 4x SDS Loading buffer that contained 50 mM EDTA and samples were separated by SDS-PAGE and transferred to nitrocellulose. Western blots were performed using the 4G10 platinum anti-phosphotyrosine antibody as a primary (Millipore) and IRDye 800CW Goat Anti-Mouse IgG antibody (Li-Cor #827-08364) as a secondary. Blots were visualized using the Li-Cor Odyssey Imaging System, and kinetic constants and their errors for reactions in the presence or absence of Ste5-FBD fragment were determined by non-linear least-squares fitting of initial rate data in R.

For the Ste5 FBD titration experiments in Figures S3B and S5B, initial rates of MAPK autophosphorylation were determined as before but reactions contained only 1 μM MAP kinase (to ensure [MAPK] < K_{act}) and variable amounts of the Ste5 FBD fragment.

Pull-Downs of Erk-like Kinases by *S. cerevisiae* Ste5-FBD

Pull-downs were performed using GST-tagged *S. cer*. Ste5-FBD as bait (or GST alone as a control) to capture ERK-like kinase preys. 100 μl of 50 μM GST-*S. cer.*-Ste5-FBD or GST was incubated with 15 μl of glutathione agarose beads (Sigma) in SKB for 30 min at room temperature to saturate the beads with bait. The unbound protein was removed, and 100 μl of 10 μM kinase prey in SKB was applied to the beads and incubated for 1 hr at 4° with gentle agitation. Following incubation, beads were washed three times with 500 μl of SKB. The bound sample was eluted by boiling the beads in the presence of 30 μl 2x SDS loading buffer. Samples corresponding to the load, unbound, and pull-down fractions were analyzed by SDS-PAGE.

Morphological Response to α Factor

S. cerevisiae strain W303 and *K. lactis* strain yLB17a (Booth et al., 2010) were used for morphological analysis as performed previously (Malleshaiah et al., 2010). For *S. cerevisiae*, an overnight culture was washed twice with distilled water to dilute Bar1 from the media and cultures were diluted to OD 0.05 in SC and grown for 4 hr at 30°. The culture was split into separate tubes and α-factor peptide (*S. cer.* -α: N-WHWLQLKPGQPMY-C) was added to the indicated concentration. After 180 min, the morphology of cells was determined by light microscopy. For *K. lactis*, an overnight culture was grown in SC, washed twice with distilled water, and grown for an additional 6 hr in SC media lacking phosphate to allow cells to become mating competent (Booth et al., 2010; Tuch et al., 2008a). The culture was split into separate tubes and α-factor peptide (*Klac*-α: N-WSWITLRPGQPIF-C) was added to the indicated concentration. After 6 hr, the morphology of cells was determined by light microscopy. For both *S. cerevisiae* and *K. lactis*, morphologies were manually determined by inspection of images in ImageJ. Unlike S. *cerevisiae*, the majority of *K. lactis* cells do not produce mating projections even under saturating doses of α-factor peptide (<30%) although the percentage of cells in the culture shmooing does indeed plateau with increasing dose. For this reason, we normalized the percentage of cells shmooing for each species to the maximum percentage of cells shmooing we observed to facilitate comparison of the two profiles.

Analysis of In Vivo Mating Behavior of Ste5 Chimeras Harboring VWA Sequences from Different Species

The ability of Ste5 chimeras harboring VWA sequences from different species to support wild-type mating in vivo was determined by a growth complementation assay. Transformants of *S. cerevisiae* strain RB201 (a ΔSte5 W303 derivative) harboring CEN/ARS plasmids expressing wild-type or chimeric Ste5 protein sequences from the native Ste5 promoter were grown overnight in SD–Ura media. Cultures were diluted to OD 0.5 and 10 μl of each culture was spotted onto SC-Ura plates and grown overnight at 30° to produce a uniform patch. To test for mating, a 10 ml culture of the MAYA12 mating tester strain (α mating type, *lys*-) was grown to OD 1.0, pelleted, and resuspended in 500 μl of YPD and plated as a lawn on a YPD agar plate. Once dry, the RB201 derivative patches were

replica-plated to the MAYA12 lawn YPD plates and allowed to mate overnight at 30°. These plates were then replica-plated to synthetical minimal media plates on which only diploids produced from MAYA12 x RB201 matings are able to grow. After 2 days, the plates were photographed for analysis.

SUPPLEMENTAL REFERENCES

Côte, P., Sulea, T., Dignard, D., Wu, C., and Whiteway, M. (2011). Evolutionary reshaping of fungal mating pathway scaffold proteins. mBiol *2*, e00230-10.

Coyle, S.M., Gilbert, W.V., and Doudna, J.A. (2009). Direct link between RACK1 function and localization at the ribosome in vivo. Mol. Cell. Biol. *29*, 1626–1634.

Felsenstein, J. (1985). Confidence limits on phylogenies: an approach using the bootstrap. Evolution *39*, 783–791.

Jones, D.T., Taylor, W.R., and Thornton, J.M. (1992). The rapid generation of mutation data matrices from protein sequences. Comput. Appl. Biosci. *8*, 275–282.

Tamura, K., Peterson, D., Peterson, N., Stecher, G., Nei, M., and Kumar, S. (2011). MEGA5: molecular evolutionary genetics analysis using maximum likelihood, evolutionary distance, and maximum parsimony methods. Mol. Biol. Evol. *28*, 2731–2739.

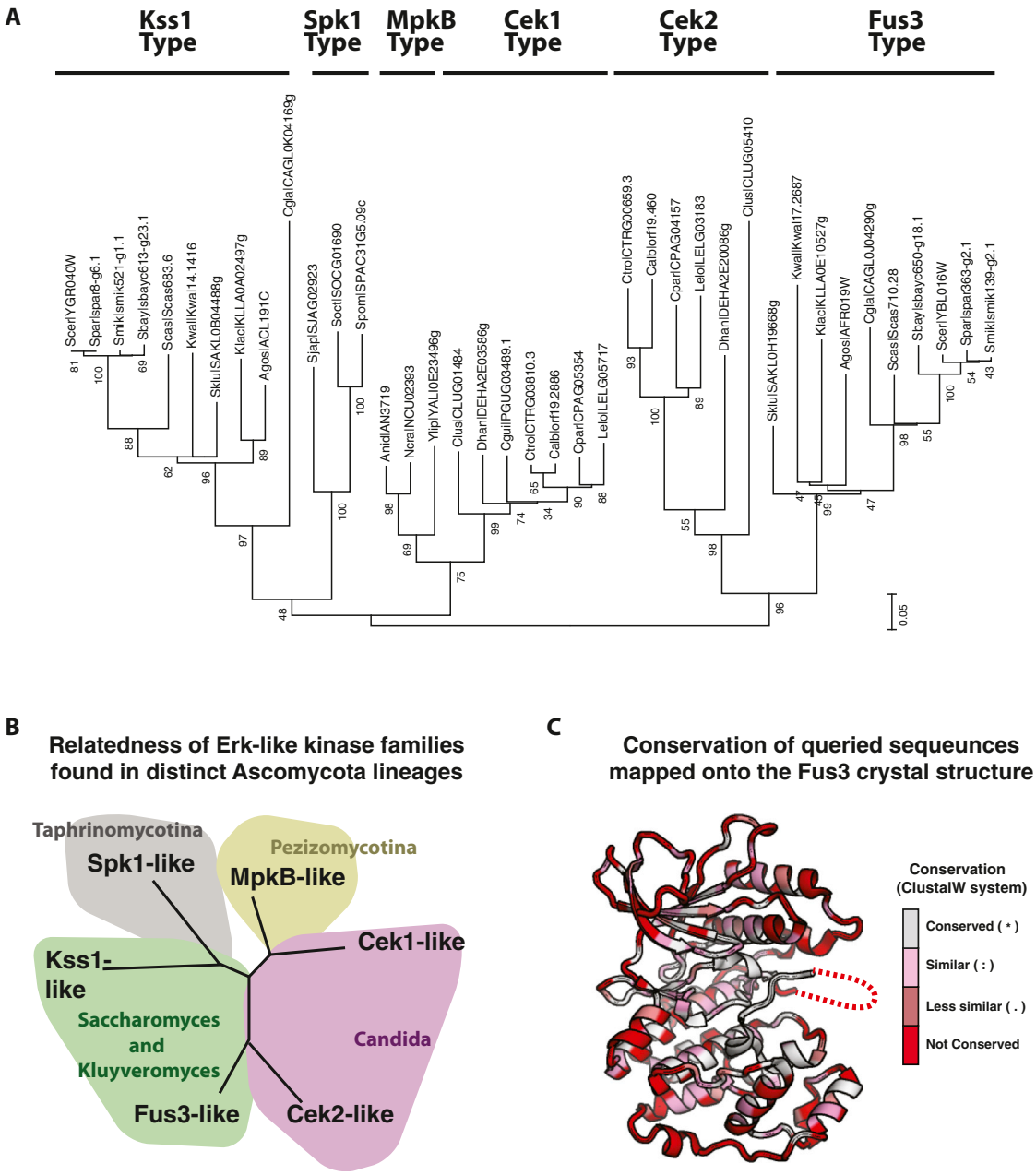

Figure S1. Additional Support that the Erk-like Kinases Are Divergent across the Ascomycota and that Distinct Erk-like Kinase Types Are Associated with Specific Fungal Lineages, Related to Figure 1

(A) The bootstrap consensus tree inferred from 500 replicates is shown and is taken to represent the evolutionary history of the ERK-like kinase taxa analyzed, as detailed in the Extended Experimental Procedures. Major branches with good bootstraps values correspond to particular kinase types found in distinct fungal lineages: Fus3 and Kss1 type kinases, found in the *Saccharomyces* and the *Kluveromyces*; Cek1 and Cek2 type kinases, found in the *Candida*; MpkB-like kinases, found in the filamentous fungi (pezizomycotina) such as *Neurospora crassa*; and Spk1-like kinases, found in taphrinomycotina such as *Schizosaccharomyces pombe*.

(B) Simplified representation of tree in (A), showing the relationship of the major kinase types and the fungal lineages that contain those kinase types.

(C) Fus3 crystal structure colored by the extent of conservation at each sequence position using the ClustalW similarity scoring system: (*) conserved, white; (:) similar, pink; (.) less similar, burgundy; ( ) no conservation, red. This coloring shows that while some elements of the hydrophobic core as well as key residues involved in catalysis are highly conserved, overall there is considerable divergence across the sequences we queried at most amino acid positions.

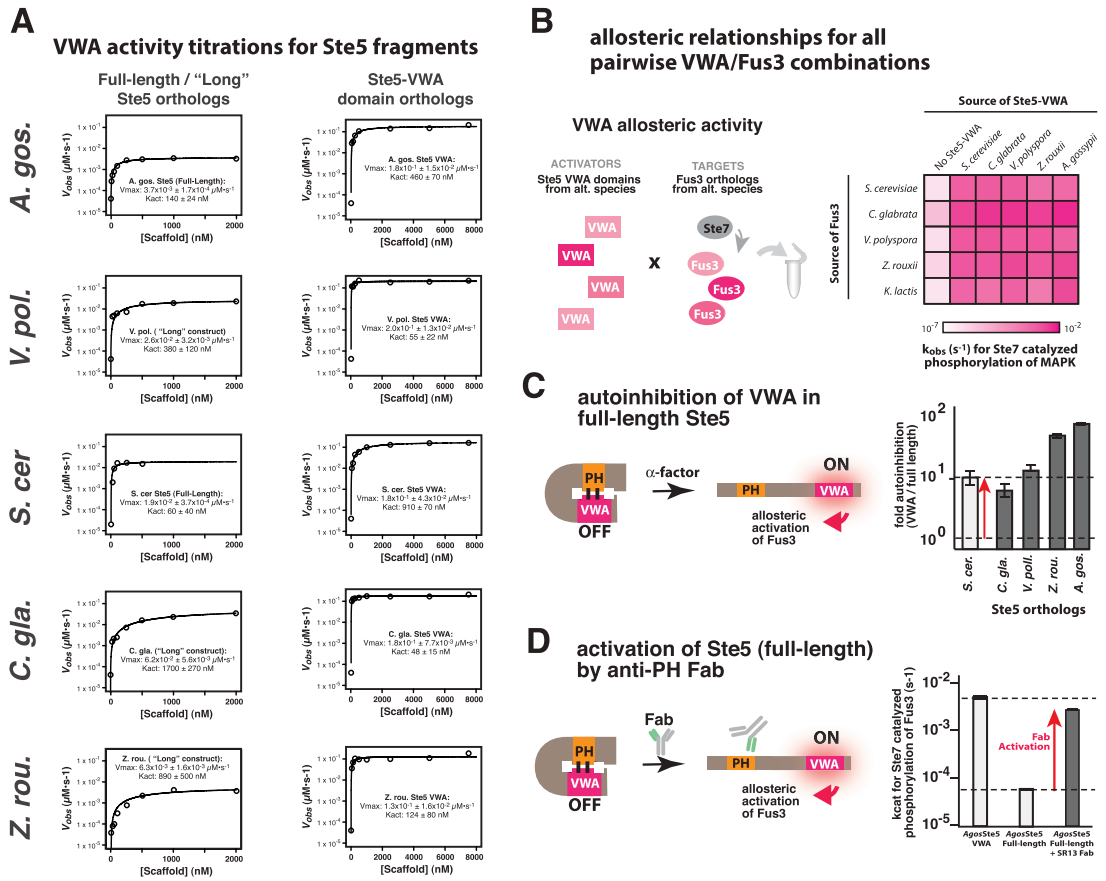

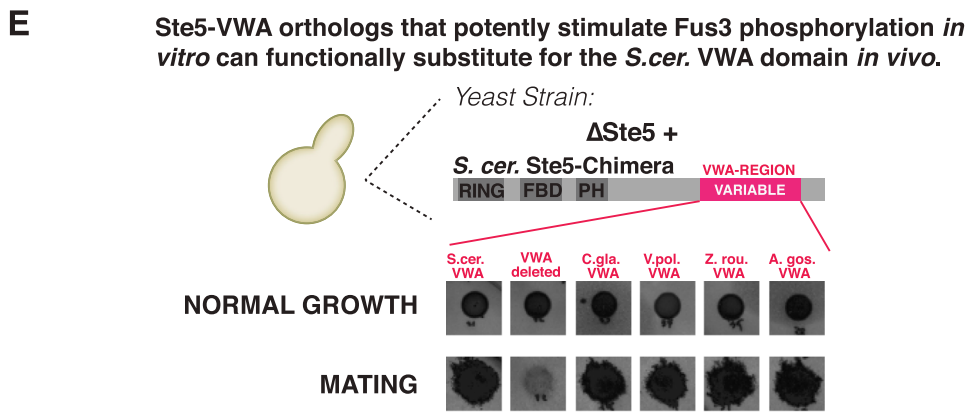

Figure S2. Additional Support that a Potent Autoinhibited Ste5-VWA Activity Is Conserved in All Fus3/Kss1/Ste5-Containing Species, Related to Figure 2

(A) Titration curves indicating the rate-enhancement for Ste7 catalyzed phosphorylation of Fus3 as a function of increasing concentrations of scaffold effector. The associated data, curves (fit to $V_{obs} = V_{max}$*[Scaffold]/([Scaffold]+K_{act})) and fit parameters for each construct are indicated.

(B) Matrix indicating the k_{cat} for Ste7 catalyzed phosphorylation of an indicated Ste5-VWA and Fus3 ortholog pairing.

(C) Rate enhancements provided by the longest Ste5 construct we could express for each ortholog relative to that of the corresponding isolated VWA domain are indicated.

(D) A Fab antibody fragment that binds to the PH domain of *S. cerevisiae* Ste5 relieves Ste5 autoinhibition (Zalatan et al., 2012). The observed rate constant for Ste7-catalyzed phosphorylation of Fus3 in the presence of 250 nM *A. gossypii* Ste5-VWA domain, 250 nM *A. gossypii* full-length Ste5, and 250 nM *A. gossypii* full-length + 2 μM Sr13 Fab antibody are indicated.

(E) Total growth and mating-dependent growth of RB201 (a ΔSte5 W303 derivative) *S. cerevisiae* strains containing Ste5 chimeras harboring VWA sequences from other species is shown. Error bars represent SEM.

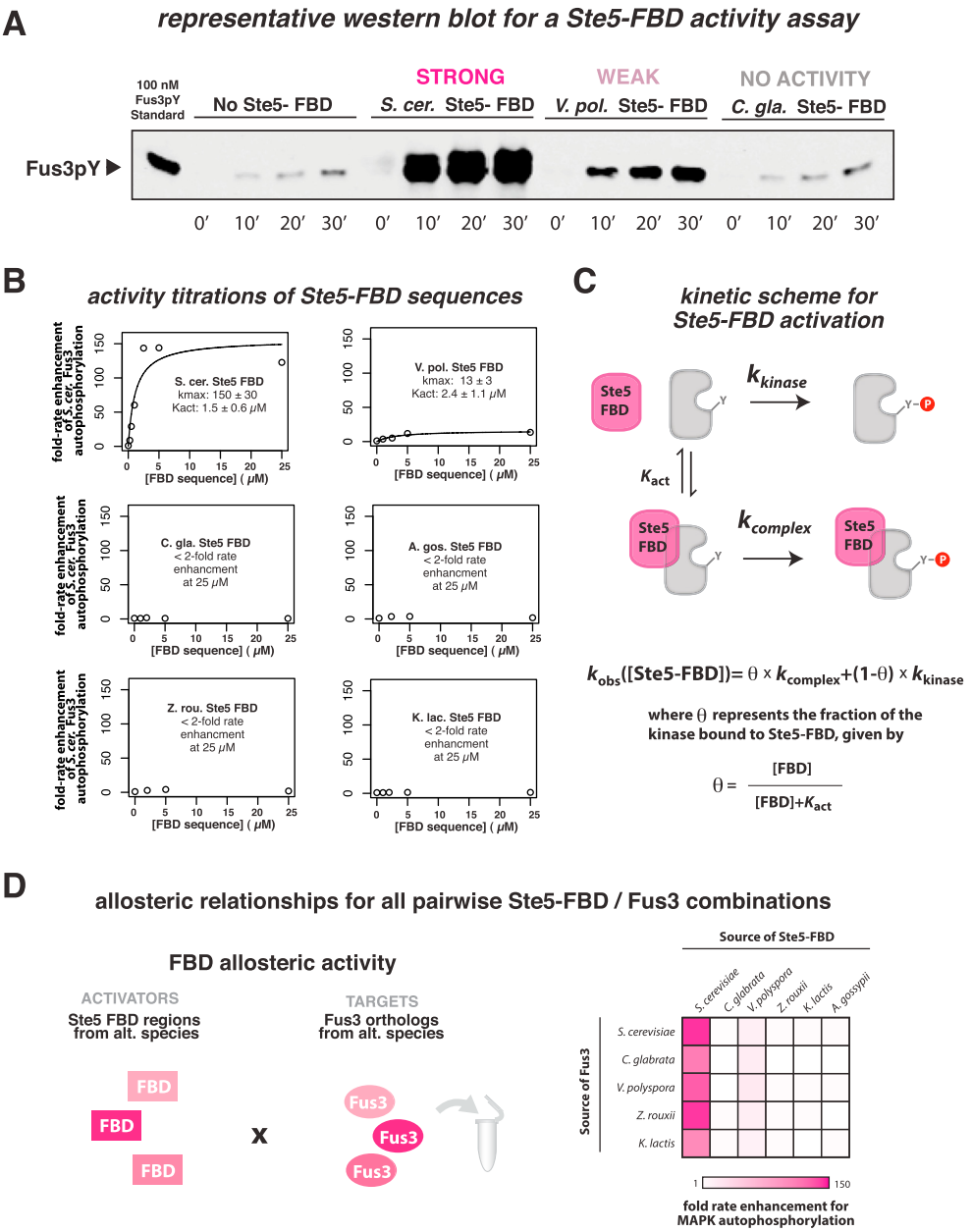

Figure S3. Additional Support that Potent Ste5-FBD Activity Is a Unique Feature of Only Select Ste5-Containing Lineages, Related to Figure 2

(A) Representative western blot showing time-courses for Fus3 autophosphorylation in either the absence of any Ste5-FBD sequence or in the presence of 25 μM of the indicated Ste5-FBD fragment.

(B) Titration curves indicating the rate-enhancement for Fus3 autophosphorylation as a function of increasing concentrations of scaffold effector. The associated data and—when appropriate—curves (fit to the equation described in (C)) and associated fit-parameters are indicated. *S. cer*. and *V. pol*. Ste5-FBD sequences differ in the maximum allosteric effect that they could exert on the kinase (maximal rate of autophosphorylation: *S. cer*.-k_{max} = 154 ± 16-fold and *V. pol*.-k_{max} = 12.8 ± 1.1-fold) and not in their apparent affinities (K_{act}, the concentration of activator required for half-maximal activation: *S. cer*.-K_{act} = 1.5 ± 0.6 μM and *V. pol*.-K_{act} = 2.4 ± 1.1 μM).

(C) Scheme for Ste5-FBD activation of Fus3 used to fit data in (B) and extract a binding parameter (K_{act}) as well as a maximal rate enhancement parameter (k_{max}).

(D) Matrix indicating the fold-rate enhancement for MAPK autophosphorylation of the corresponding Ste5-FBD and Fus3 orthologs. Ste5-FBD activity appears to be absent from the majority of species tested and the allosteric features that *S. cer*. Ste5-FBD and *V. pol*. Ste5-FBD act on is present in all Fus3 orthologs to a comparable degree, even when no Ste5-FBD activity is present in that species.

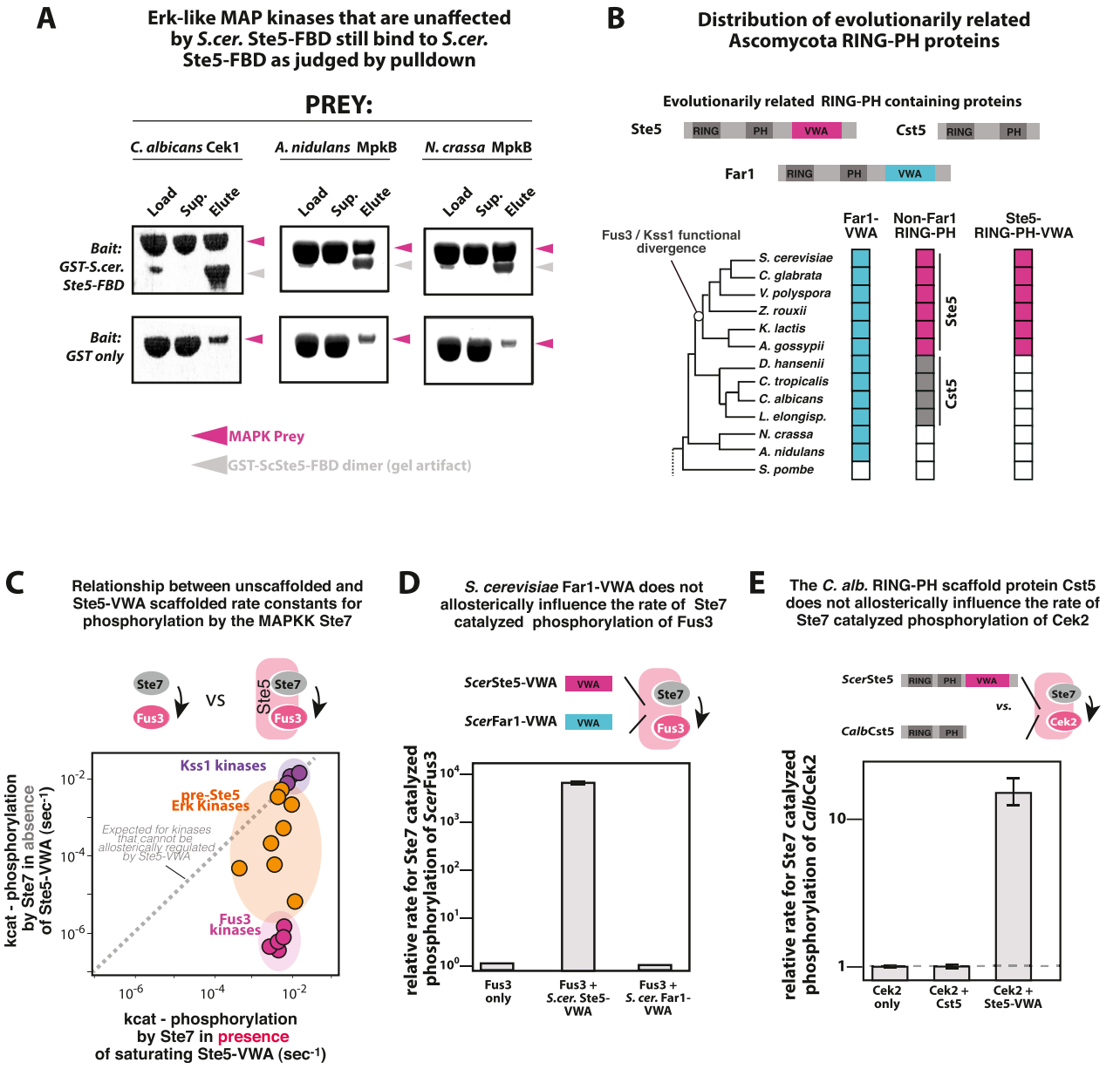

Figure S4. Additional Support for a Latent and Drifting Capacity for Allosteric Regulation by Ste5-FBD and Ste5-VWA in the Pre-Ste5 Erk-like MAP Kinases, Related to Figure 4

(A) GST pull-downs showing the extent of *S. cer*. Ste5-FBD binding to the indicated Erk-like kinases that did not respond to allosteric regulation by *S. cer*. Ste5-FBD.

(B) Distribution of RING-PH containing proteins that are evolutionarily related to Ste5 across the Ascomycota. Far1 orthologs were identified in all species except *S. pombe*; Cst5 orthologs were identified only in species within the *Candida* (CTG) clade; only the *Saccharomyces* and *Kluveromyces* clades were found to contain Ste5 RING-PH-VWA orthologs. This analysis is similar to that of a previously study (Côte et. al., 2011).

(C) Relationship between rate constants for Ste7 catalyzed phosphorylation of an Erk-like MAP kinase in the presence or absence of the *S. cer*. Ste5-VWA domain. Circles in the plots correspond to individual MAP kinases (Fus3-type kinases: pink; Kss1-type kinases: purple; pre-Ste5 Erk-like kinases: orange) that we examined and indicate their associated properties. The gray dotted line indicates where kinases would be expected to be distributed if they were not responsive to Ste5-VWA allosteric regulation.

(D) The rate constants for Ste7 catalyzed phosphorylation of *S. cer*. Fus3 under the indicated conditions are shown. *S. cer*. Far1-VWA does not appear to stimulate phosphorylation of Fus3, suggesting VWA domains from Far1 do not possess cryptic allosteric activity. Error bars represent SEM.

(E) Rate constants for Ste7 catalyzed phosphorylation of Cek2 under the indicated conditions are shown. *S. cer*. Ste5-VWA, but not Cst5, stimulated phosphorylation of *C. alb*. Cek2 by ~12-fold.

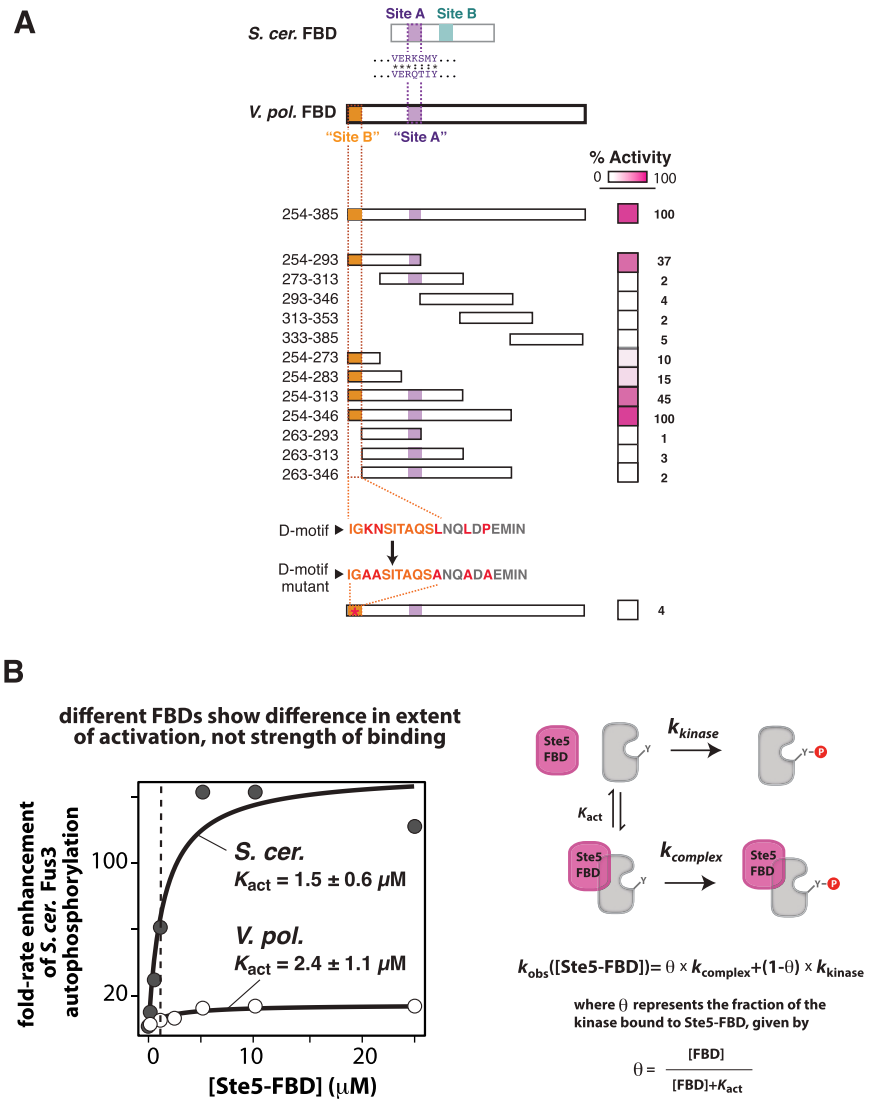

Figure S5. Additional Biochemical Dissection of the *V. pol*. Ste5-FBD Activation Mechanism, Related to Figure 5

(A) Additional truncation mapping data for the *V. pol*. Ste5-FBD fragment, showing the relative activity of an indicated truncation or fragment.

(B) Comparison of *S. cer*. and *V. pol*. Ste5-FBD titration profiles for the rate-enhancement of Fus3 autophosphorylation. Data were fit to the indicated model to extract K_{act} and k_{max} parameters. These two motifs differed in the maximum allosteric effect that they could exert on the kinase (maximal rate of autophosphorylation: *S. cer*.-k_{max} = 154 ± 16-fold and *V. pol*.-k_{max} = 12.8 ± 1.1-fold) and not in their apparent affinities (K_{act}, the concentration of activator required for half-maximal activation: *S. cer*.-K_{act} = 1.5 ± 0.6 μM and *V. pol*.-K_{act} = 2.4 ± 1.1 μM).